Study of Spatial Inhomogeneities in Swollen Latex Particles by Small-Angle X-ray Scattering: The Wall-Repulsion Effect Revisited

J. Bolze and M. Ballauff*

Polymer-Institut, Universität Karlsruhe, Kaiserstrasse 12, 76128 Karlsruhe, Germany

Received April 18, 1995; Revised Manuscript Received August 8, 1995®

ABSTRACT: A small-angle X-ray scattering (SAXS) study of PMMA-latex particles swollen with methyl methacrylate (MMA) is presented. The electron density of the swollen particles can easily be matched by addition of sucrose to the latex. Also, there is an excellent contrast between the polymer and its monomer. SAXS measurements in conjunction with contrast variation near the match point are therefore well-suited for the detection of even minute changes of the radial concentration profile. Thus, this method is capable of detecting the depletion of the polymer chains near the particle surface due to the wall-repulsion effect. The results point to an outer shell of approximately 2 nm thickness in which the swelling agent is enriched. It is concluded that the present system exhibits a small but non-negligible wall-repulsion effect which is discussed in terms of recent theoretical approaches to the problem.

Introduction

Most current treatments of the kinetics of emulsion polymerization assume a homogeneous polymer segment density distribution within the growing latex particle. On the other hand, the radius of the latex particles typically obtained from emulsion polymerization is on the same order of magnitude as the radius of gyration of high molecular weight polymers. If such a particle is swollen by a solvent, the confined polymer chains will tend to avoid the particle surface for entropic reasons. This "wall-repulsion effect" first discussed in detail by Casassa[1,2] and by de Gennes[3,4] therefore will lead to a decrease in polymer concentration near the particle surface.

The treatment by Casassa[5,6] models a single random-flight chain confined inside a spherical cavity and predicts a marked depletion of the segment density at the wall (cf. Figure 5 of ref 5). Croxton et al.,[7] however, have argued that this calculation overestimates the depletion effect since it neglects interactions between different chains at finite polymer concentrations. Thus these workers drew the conclusion that the wall-repulsion effect in swollen latex particles is rather marginal and restricted to the immediate neighborhood of the particle surface.

The influence of the polymer concentration has been modeled quantitatively by Ronca[8] and by Scheutjens and Fleer.[9] Both treatments show that at high polymer concentrations the repulsive effect at a solid nonadsorbing wall will be screened considerably so that the decrease in segment density near the boundary will be much less marked than in the case of dilute solutions. An analytical expression for the depletion layer thickness as a function of the bulk polymer concentration has been developed by Vincent.[10] It is determined by the balance of the wall-repulsion effect and the osmotic pressure of the bulk polymer solution. For the high polymer concentrations typical for swollen latex particles this model also predicts a rather weak depletion effect of a few nanometers only. Brazhnik et al.[11] developed a theory for the segment concentration profile near a solid wall in polymer melts.

Recently, Evers, Ley, and Hädicke[12,13] extended the Scheutjens–Fleer approach for modeling polymer/monomer particles in solution. Their results also point to a rather thin depletion layer. In addition to this, their model allows the discussion of enthalpic effects which may modify the local structure at the surface of the polymer particles and even counterbalance the wall-repulsion effect.

An additional argument against a strong wall-repulsion effect is related to the "surface anchoring effect": When a water-soluble initiator is used, the polymer chains will bear polar headgroups as, e.g., $-SO_4^-$, which will affix at least one end of the chains on the particle surface[14,15] and thus counteract the depletion of polymer segments.

Only a few experimental studies on the wall-repulsion effect in latex particles have been published so far. Linné et al.[16] and Yang et al.[5] extracted the single chain form factor of the polymer chains in latex particles using small-angle neutron scattering (SANS). They concluded that the wall-repulsion effect was quite pronounced for certain ratios of the radius of gyration of the polymer chains to the particle size.

Recently, Mills et al.[17] came to different results by a set of well-designed experiments: In a first series, a polystyrene latex was swollen with perdeuteriotoluene. The form factor of the swollen particles was determined at different contrasts through SANS. The results obtained by this experiment pointed to a homogeneous density within the swollen particles. In a second set of experiments, protonated particles were swollen with deuterated monomer to equilibrium and subsequently polymerized. Here the scattering intensities, in particular at low contrast, showed that the resulting particles exhibit a core–shell structure mainly originating from the surface anchoring effect.

The foregoing brief overview shows that theoretical arguments as well as experimental data have not come to a definite answer regarding the extent of spatial inhomogeneities in swollen latex particles yet. Obviously, a highly precise investigation of the radial structure by a scattering method would be very helpful,

* To whom all correspondence should be addressed.

® Abstract published in *Advance ACS Abstracts,* October 1, 1995.

0024-9297/95/2228-7429$09.00/0

but it is necessary to extend the resolution and the sensitivity of the experiment down to the scale of a few nanometers.

In recent publications[18-22] we have shown that small-angle X-ray scattering (SAXS) is nearly ideally suited for the study of the radial structure of latex particles. The match point where the electron densities of the particles and the dispersion medium are equal may easily be reached for common polymers like polystyrene or PMMA by adding sucrose.[19,20] Thus a detailed study of the radial electron density distribution using contrast variation[23-30] can be conducted.

In this work we use contrast variation near the match point to investigate the radial structure of PMMA-latex particles swollen by MMA. This particular swelling agent has been chosen since it has a much lower electron density than PMMA (PMMA, 383.4 electrons/nm^3; MMA, 305.3 electrons/nm^3; H_2O, 333.3 electrons/nm^3). Thus, there is a marked contrast as a function of the polymer concentration and minute variations of the radial concentration profile become detectable. Another reason for choosing this system is the direct applicability of the results to seeded emulsion polymerization of MMA onto PMMA seed particles (cf. the discussion of this point in ref 20).

Experimental Section

Materials. The monomer MMA (Fluka) was washed with 10 wt % aqueous sodium hydroxide solution, followed by water, dried overnight at 4 °C over anhydrous $CaCl_2$, and subsequently distilled under reduced pressure in a N_2 atmosphere. Distilled water was freed from dust through a filter funnel (pore diameter ca. 1.5 μm). The initiator $K_2S_2O_8$ (Fluka) was recrystallized twice from water at 30 °C and then dried at ambient temperature under reduced pressure. The surfactant sodium dodecanesulfonate (SDS, Lancaster) as well as the inhibitor hydrochinon (Fluka) were used as received.

Emulsion Polymerization. The PMMA latex was prepared by a conventional batch process under an atmosphere of nitrogen using a 1 L glass reactor equipped with a reflux condensator, a sampling tube, a thermometer, and a paddle-type Teflon stirrer. The following recipe was used: MMA, 200 g; H_2O, 726 g; SDS, 1.99 g; $K_2S_2O_8$, 1.20 g.

Polymerization was started by addition of the initiator dissolved in 20 mL of water. The reaction was run at 60 °C at a constant stirring speed of 300 rpm. During the last hour the temperature was raised by 10 deg. Inhibitor solution was injected after 7 h, and the reactor was cooled in an ice-water bath to ambient temperature. The solid content was determined gravimetrically to 22 wt %, which means that the conversion was practically 100%.

Since the swelling of the particles leads to a marked increase in the surface area, an additional surfactant solution (sodium dodecylbenzenesulfonate, SDBS) was added to the latex in order to avoid coagulation. It could be shown that the surface coverage was inconsequential for the SAXS analysis of the PMMA latex under consideration. The surface coverage by surfactant was approximately 90% before swelling; then MMA stabilized by 1‰ hydroquinone was cautiously added to the latex with gentle shaking. The MMA added amounted to 62 vol % of the PMMA in the latex. Swelling equilibrium was achieved after a rather short time (less than 3 h) since the SAXS measurement of the sample after 18 h led to the same result as the one determined after 3 h.

The density of the swollen latex particles was determined by the DMA-60 apparatus (Paar KG, Graz, Austria) to be 1.132 g/cm^3.

Small-Angle X-ray Scattering. SAXS measurements were done in the q range of 0.08 nm^{-1} < q < 5 nm^{-1} ($q = (4\pi/\lambda)\sin(\theta/2)$; θ, scattering angle; λ, wavelength of the Cu Kα radiation used in the experiment) using a Kratky-Kompakt-Kamera (Paar KG, Graz, Austria) equipped with a position-sensitive detector (Braun, Germany). All samples were measured at a constant temperature of 298 K. The details of the experimental procedures and of the subsequent data treatment are given in refs 18,19.

For contrast variation the electron density of the dispersion medium was raised by adding D(+)-sucrose (Fluka >98%; used without further purification). The densities of the sucrose solutions were measured using the DMA-60 apparatus. The number of electrons/nm^3 (ρ_m) of the dispersion medium follows as $\rho_m = 332.39 + 1.31c$, where c denotes the weight percentage of sucrose in the respective solution. Dilution was effected with 0.01 mol/L KCl solution.

Theory

For a dilute system of monodisperse particles the intensity per volume normalized to the scattering intensity of a single electron (e.u./nm^3) follows as (cf. refs 19,31)

$$I(q) = NB^2(q) \tag{1}$$

where N is the number of particles per unit volume and $B(q)$ is the scattering amplitude. For spherical symmetric particles with radius R, $B(q)$ is given by

$$B(q) = 4\pi\int_0^R[\rho(r)-\rho_m]r^2\frac{\sin(qr)}{qr}\,dr \tag{2}$$

with $\rho(r)$ being the local electron density in the particles and ρ_m the respective value of the dispersion medium.

With definition of the volume-average $\bar{\rho}$ of the electron density of the particles

$$\bar{\rho} = \frac{4\pi\int_0^R \rho(r)r^2\,dr}{4\pi\int_0^R r^2\,dr} \tag{3}$$

the local density $\rho(r)$ may be rendered as

$$\rho(r) = \bar{\rho} + \Delta\rho(r) \tag{4}$$

and the scattering amplitude is split into two parts:

$$B(q) = B_0(q) + \epsilon(q) \tag{5}$$

with

$$B_0(q) = (\bar{\rho} - \rho_m)4\pi\int_0^R\frac{\sin(qR)}{qR}r^2\,dr \tag{6}$$

and

$$\epsilon(q) = 4\pi\int_0^R\Delta\rho(r)\frac{\sin(qr)}{qr}r^2\,dr \tag{7}$$

For the subsequent discussion it is instructive to note that $B_0(q)$ refers to the scattering amplitude of a homogeneous sphere of electron density $\bar{\rho}$ whereas $\epsilon(q)$ accounts for the contribution due to internal variations of the electron density. Thus studies of the fine radial structure must be conducted near the match point, since otherwise the form part $B_0(q)$ will dominate the scattering intensity and hide the weak contribution of the internal variation of the electron density.

On the other hand, measurements around the match point are rather difficult since a thin shell, for example, leads only to a small internal contribution $\epsilon(q)$. In this case only if the signal-to-background ratio is good enough will measurements lead to meaningful results.

The above equations furthermore show[31] that for values of q satisfying $q^*R = \tan(q^*R)$ the amplitude $B_0(q)$ is zero for all contrasts and then the scattering intensity is solely given by $\epsilon(q^*)$. Since $\epsilon(q)$ does not depend on contrast, all scattering intensities of uniform systems must intersect at $q = q^*$.

For polydisperse systems the measured size distribution of the latex particles is needed for the calculation of the scattering intensity through[26,28,31]

$$I(q) = \sum_i N_i B_i^2(q) \tag{8}$$

where the index i refers to the particles of radius r_i. As outlined previously,[18,19] the size distribution of the latex particles was modeled using a slightly asymmetric distribution as measured by ultracentrifugation.[32]

Model Calculations

The various theoretical analyses of the wall-repulsion effect discussed in the Introduction suggest that the range of spatial inhomogeneities may be rather small and restricted to the immediate vicinity of the interface between the particle and the water phase. It is therefore instructive to calculate theoretical scattering curves as a function of contrast for a polydisperse system of spheres exhibiting only a marginal wall-repulsion effect.

We first discuss the effect of a thin shell in polydisperse particles ($D_w/D_n = 1.041$) with an asymmetric size distribution[18,19] as mentioned above and a number-average diameter of $D_n = 74$ nm. It is assumed that the electron density decreases linearly by 20 nm^{-3} within an outer shell of 3 nm (see Figure 1a). The resulting scattering intensities calculated with (1), (2), and (8) are shown in Figure 1b. Figure 1b shows that with decreasing contrast the extrema of the curves are slightly shifted toward higher q values. Near the match point there is a sudden shift toward the ordinate. In case of negative contrast ($\bar{\rho} < \rho_m$) the extrema are shifted to higher q values again. A further increase of the electron density in the dispersion medium will lead to the dominance of the form contribution $B_0(q)$ to the scattering intensity and hide the fine details of the radial density distribution. Only in this limit of high contrast are the positions of the extrema practically constant, and the scattering curves will just be shifted vertically with contrast, which is also a typical characteristic of homogeneous spheres.

For a system of monodisperse spheres with $\rho(r)$ given by the profile shown in Figure 1a, all scattering curves would cross at certain values q^*, as discussed above. But for polydisperse systems the extrema are smeared out and, consequently common points of intersection cannot be observed.

For further discussion of our SAXS analysis of swollen particles, it is instructive to model the effect of a thin layer with a *higher* electron density than the core. Such a layer could be due to a surfactant adsorbed on the surface of the particle.[18]

Figure 2 shows the resulting calculated scattering curves for particles with a radial electron density increasing linearly by 20 nm^{-3} from the core value within 3 nm (cf. inset of Figure 2). The scattering intensities (Figure 2) were modeled with the same size distribution ($D_w/D_n = 1.041$) of the particles as above and with a number-average diameter of $D_n = 74$ nm. The scattering intensities exhibit features similar to those in Figure 1b. However, when Figure 2 is compared to Figure 1b, the decisive difference is the direction of the shift of the extrema along the abscissa above and below the match point with varying contrast. In our second model calculation it is just the other way around. The model calculations therefore demonstrate that in this way a depleted layer near the particle

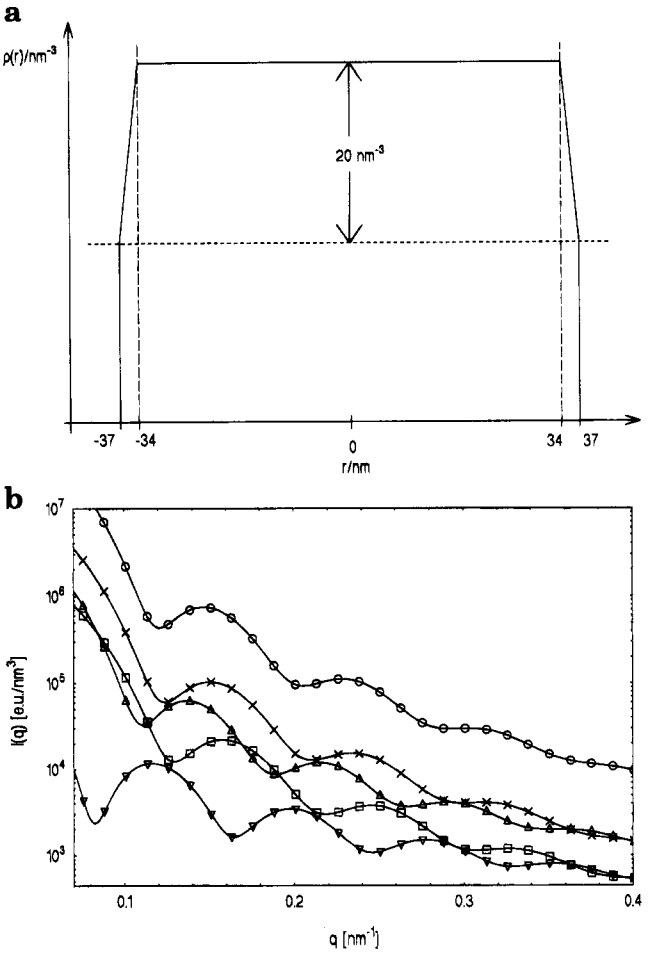

Figure 1. (a) Radial electron density profile assumed for modeling the wall-repulsion effect in latex particles. The electron density decreases by 20 nm^{-3} within a thin layer at the surface. (b) Scattering intensities calculated at different contrasts for polydisperse latex particles with the electron density profile shown in Figure 1a. The curves refer to the following contrasts, $\Delta\rho = \bar{\rho} - \rho_m$/nm^{-3}: (○) 47.7; (×) 17.7; (□) 7.7; (▽) −2.3 (hollow sphere); (△) −12.3.

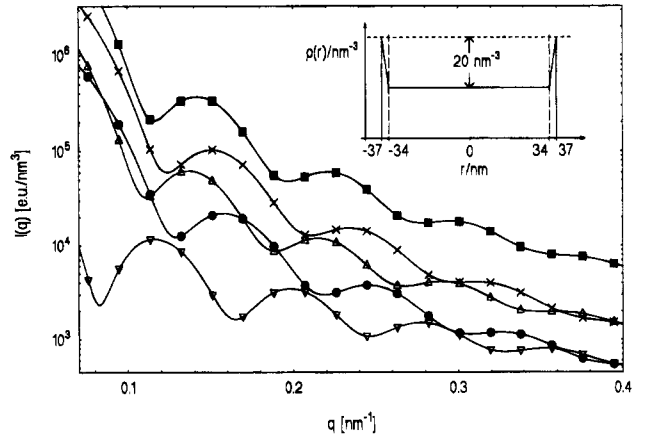

Figure 2. Scattering intensities calculated at different contrasts for polydisperse latex particles with the electron density profile shown in the inset. The curves refer to the following contrasts, $\Delta\rho = \bar{\rho} - \rho_m$/nm^{-3}: (■) 32.3; (△) 12.3; (▽) 2.3 (hollow sphere); (●) −7.7; (×) −17.7.

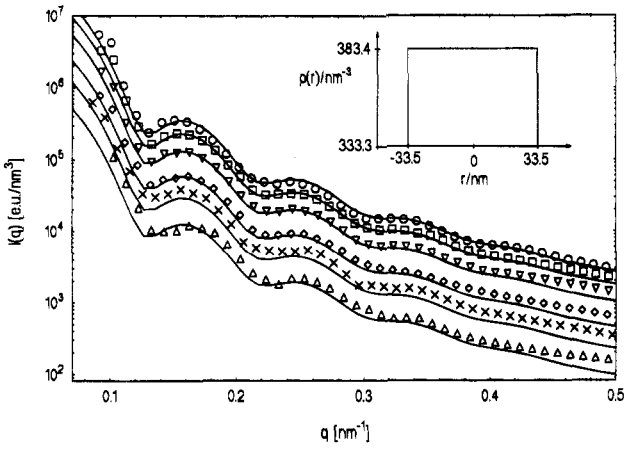

Figure 3. SAXS intensities of the unswollen PMMA-latex particles. The solid lines refer to the fit curves calculated by assuming a homogeneous electron density within the particles (see inset). The following numbers refer to the content (wt %) of sucrose in the dispersion medium whereas the numbers in parentheses denote the contrast, $\Delta\rho = \rho - \rho_m/\mathrm{nm}^{-3}$: (○) 0% (50.1); (□) 8% (40.7); (▽) 16% (30.8); (◇) 24% (20.9); (△) 32% (9.5); (×) 50% (−15.4).

surface having a lower electron density can unambiguously be distinguished from a layer with a higher electron density than the core.

Results and Discussion

Unswollen Latex. We first discuss the scattering pattern of the unswollen PMMA latex measured at positive and negative contrasts. The experimental scattering intensities could be modeled in terms of a system of homogeneous spheres having the electron density of solid PMMA. As mentioned above, the size distribution was assumed to be slightly asymmetric.[18,19] Taking a Gaussian distribution instead would lead to worse fits in agreement with previous findings. The fit which was achieved with a consistent set of fit parameters is shown in Figure 3. It gives a number-average diameter D_n of 67.0 nm and a polydispersity expressed by $D_w/D_n = 1.049$.

The good fit of the experimental scattering intensities and in particular the parallel shift of all curves with decreasing contrast (cf. ref 19) immediately shows that the unswollen PMMA particles can be regarded as homogeneous spheres. Only at lowest contrast ($\Delta\rho$ = 9.5 nm^{-3}) is the fit slightly poorer, which may be interpreted in terms of a very thin shell of a size below 1 nm. It is obvious, however, that such small deviations can be caused by irregularities on the particle surface.

For the PMMA latex under consideration no change in the scattering intensities could be observed when the surface coverage by the surfactant was increased to 80%. Therefore the amount of added surfactant is of no concern for the analysis of the present data (but see the discussions of this point in ref 18).

Swollen Latex. Figure 4a,b shows the scattering intensities of the swollen latex measured at eight different contrasts above and below the match point. The characteristic shift of the maxima away from the ordinate with decreasing contrast immediately points to the existence of a layer near the particle interface in which there must be a decrease in the electron density (cf. Figure 1a,b).

The scattering intensities of the swollen particles as displayed in Figure 4a,b were fitted now using the same type of electron distribution as shown in Figure 1a. Here

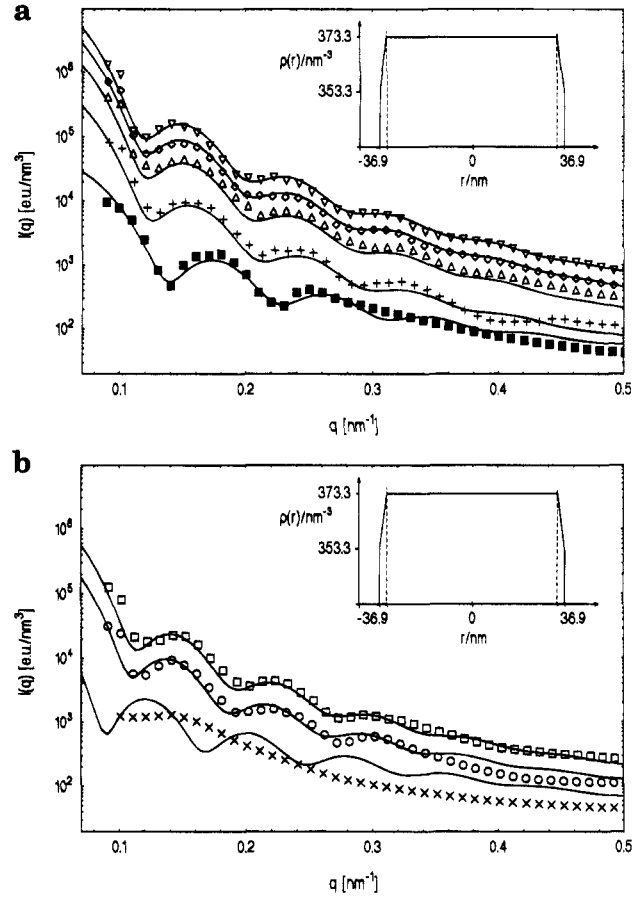

Figure 4. (a) SAXS intensities of the swollen PMMA-latex particles at positive contrasts. The solid lines refer to the fit curves calculated by assuming the radial electron density shown in the inset (shell thickness 2.2 nm). The following numbers refer to the content (wt %) of sucrose in the dispersion medium whereas the numbers in parentheses denote the contrast, $\Delta\rho = \rho - \rho_m/\mathrm{nm}^{-3}$: (▽) 0% (38.3); (◇) 8% (28.9); (△) 16% (19.0); (+) 24% (8.7); (■) 28% (2.0). (b) SAXS intensities of the swollen PMMA-latex particles at negative contrasts. The solid lines refer to the fit curves calculated by assuming the radial electron density shown in the inset (2.2 nm shell thickness). The following numbers refer to the content (wt %) of sucrose in the dispersion medium whereas the numbers in parentheses refer to the contrast, $\Delta\rho = \rho - \rho_m/\mathrm{nm}^{-3}$: (×) 32% (−2.3); (○) 36% (−8.5); (□) 40% (−14.1).

the electron density of the core decreases by 20 nm^{-3} within an outer shell of 2.2 nm (cf. inset of Figure 4). The scattering intensities calculated with this profile (eq 2) are shown by the solid curves in Figure 4a,b. Good agreement between the fitted curves and the experimental data can be seen; only in the case of very low contrast (32% sucrose; Figure 4b) could the scattering intensities not be determined with sufficient resolution, but at least the measurements coincide with the calculated intensities with regard to the order of magnitude.

The fit gives a number-average radius of the particles of 36.9 nm and an average electron density of 371.6 nm^{-3}. The latter value is considerably lower than the corresponding figure for solid PMMA (383.4 nm^{-3}), as expected for a concentrated solution of this polymer in MMA. From mass balance one would expect a radius of 39.3 nm and a concomitantly lower electron density. It has to be kept in mind, however, the MMA exhibits a rather high solubility in water (0.159 mol/L[33]) and therefore only a part of the swelling agent will enter the particles. The enhanced activity of MMA in the small spheres will furthermore decrease its concentration in the latex, and a certain part of the MMA might

have evaporated under the condition given in the experiment. Mills et al.[17] have reported the same discrepancy in the course of their studies.

A *decrease* of the electron density in the outer shell means that the monomer which has the lower electron density must be enriched there whereas the polymer chains are depleted from this region.

Attempts to evaluate the surface of the particles from the final slope of the scattering curves by Porod's law[28] did not lead to satisfying results. This is due to the fact that the scattering background of the sucrose solutions is quite high and the error induced by subtraction of this contribution may be appreciable in this region of scattering angles. The variation of the scattering curves with contrast as discussed above, however, is fully sufficient to detect small variations of the internal electron density.

Conclusion

The data presented in Figure 4a,b in conjunction with the model calculations (Figures 1 and 2) clearly point to the existence of a polymer-depleted layer near the particle surface in qualitative agreement with theoretical deductions. Its magnitude is considerably lower than suggested by the random flight model[1,2,5] but corroborates the calculations[7-13] taking into account the finite concentration of the polymer in the swollen particle. However, it is questionable whether the wall-repulsion effect can be held solely responsible for the observation reported herein. The work of Evers et al.[12,13] is particularly revealing in this respect since these workers show that the interaction parameters between the respective component in the swollen latex system have a profound influence on the morphology as well. When looking at a length scale of 1−2 nm, the interface between the particles and the water phase should not be regarded as an impenetrable wall which totally deflects the polymer chains. Hence, modeling the internal structure of swollen latex particles should take into account the finite width of the surface layer of the latex particles.

Acknowledgment. Financial support by the Deutsche Forschungsgemeinschaft, by the Bundesministerium für Forschung und Technologie (Pilotprojekt "Mesoskopische Systeme"), and by the AIF (project 9749) is gratefully acknowledged. The authors are indebted to Dr. O. G. Evers and Dr. G. Ley for helpful discussions.

References and Notes

(1) Casassa, E. F. *J. Polym. Sci., Polym. Lett. Ed.* **1967**, *5*, 773.
(2) Casassa, E. F.; Tagami, Y. *Macromolecules* **1969**, *2*, 14.
(3) de Gennes, P.-G. *Macromolecules* **1981**, *14*, 1637.
(4) de Gennes, P.-G. *Adv. Colloid Interface Sci.* **1987**, *27*, 189.
(5) Yang, Se-In; Klein, A.; Spherling, L. H.; Casassa, E. F. *Macromolecules* **1990**, *23*, 4582.
(6) Dabdub, D.; Klein, A.; Sperling, L. H. *J. Polym. Sci., Polym. Phys.* **1992**, *30*, 787.
(7) Croxton, C. A.; Mills, M. F.; Gilbert, R. G.; Napper, D. H. *Macromolecules* **1993**, *26*, 3563.
(8) Ronca, G. *J. Appl. Polym. Sci.* **1987**, *33*, 2623.
(9) Scheutjens, I. M. H. M.; Fleer, G. J. *Adv. Colloid Interface Sci.* **1982**, *16*, 361.
(10) Vincent, B. *Colloid Surf.* **1990**, *50*, 241.
(11) Brazhnik, P. K.; Freed, K. J.; Tang, H. *J. Chem. Phys.* **1994**, *101*, 9143.
(12) Evers, O. A.; Ley, G.; Hädicke, E. *Macromolecules* **1993**, *26*, 2885.
(13) Evers, O. A.; Hädicke, E.; Ley, G. *Colloid Surf., A* **1994**, *90*, 135.
(14) Chern, C. S.; Poehlein, G. W. *J. Polym. Sci., Polym. Chem. Ed.* **1987**, *25*, 617.
(15) Chang, H. S.; Chen, S. A. *Makromol. Chem. Rapid Commun.* **1987**, *8*, 297.
(16) Linné, M. A.; Klein, A.; Sperling, L. H.; Wignall, G. D. *J. Macromol. Sci., Phys.* **1988**, *B27*, 181.
(17) Mills, M. F.; Gilbert, R. G.; Napper, D. H.; Rennie, A. R.; Ottewill, R. H. *Macromolecules* **1993**, *26*, 3553.
(18) Grunder, R.; Urban, G.; Ballauff, M. *Colloid Polym. Sci.* **1993**, *271*, 563.
(19) Dingenouts, N.; Ballauff, M. *Acta Polym.* **1993**, *44*, 178.
(20) Dingenouts, N.; Kim, Y. S.; Ballauff, M. *Colloid Polym. Sci.* **1994**, *272*, 1380.
(21) Dingenouts, N.; Pulina, T.; Ballauff, M. *Macromolecules* **1994**, *27*, 6133.
(22) Ballauff, M. *Macromol. Symp.* **1994**, *87*, 93.
(23) Stuhrmann, H. B.; Kirste, R. G. *Z. Phys. Chem.* **1965**, NF *46*, 247.
(24) Stuhrmann, H. B.; Kirste, R. G. *Z. Phys. Chem.* **1967**, NF *56*, 334.
(25) Kirste, R. G.; Stuhrmann, H. B. *Z. Phys. Chem.* **1967**, NF *56*, 338.
(26) Feigin, L. A.; Svergun, D. I. *Structure Analysis by Small-Angle X-Ray and Neutron Scattering*; Plenum Press: New York, 1987.
(27) Bootle, G. A.; Lye, J.; Ottewill, R. H. *Makromol. Chem. Macromol. Symp.* **1990**, *35/36*, 29.
(28) Glatter, O.; Kratky, O. *Small Angle X-Ray Scattering*; Academic Press: London, 1982.
(29) Duits, M. H. G.; May, R. P.; de Kruif, C. G. *J. Appl. Crystallogr.* **1990**, *23*, 366.
(30) Penders, M. H. G. M.; Vrij, A. *Colloid Polym. Sci.* **1990**, *268*, 823.
(31) Philipse, A. P.; Smits, C.; Vrij, A. *J. Colloid Interface Sci.* **1989**, *129*, 335.
(32) Müller, H.-G. *Colloid Polym. Sci.* **1989**, *267*, 1113.
(33) Sütterlin, N. In *Polymer Colloids Part II*; Fitch, R. M., Ed.; Plenum Press: New York, 1980.

MA950522C